Term Paper: Flat Optics using Metasurfaces

PH4107: ADVANCED ELECTRICITY, MAGNETISM AND OPTICS

(Dated: July 11, 2025)

Nimish Sharma
21MS184

Instructor: Dr. Nirmalya Ghosh

CONTENTS

LIST OF FIGURES

Abstract: Flat optics composed of subwavelength-spaced optical scatterers— also known as metasurfaces or meta-optics, are key enabling tools for structured light not only for their compact footprint but also because of their versatility and custom design. The motivation behind the field's progress has been the new age of nano-materials and the increasing demand for control of light properties. Spin optics serve as a path to control the property of electromagnetic (EM) waves where the spin angular momentum (SAM) uplifts the degeneracy due to gradient on metasurfaces. The spin optics and metamaterials coalition has opened up a regime of spin-controlled nanophotonic applications based on the properties of metasurfaces. In addition, metasurfaces have allowed us to manipulate the optical spin-hall effect (OSHE), enabling more degrees of freedom (DOF) in controlling the wavefront.

I. INTRODUCTION

Throughout the evolution of human beings, we have always been inclined towards harnessing the properties of light since it defines how we experience the world around us. Controlling light beams has been of immense importance due to the enormous amount of information that can be perceived. Conventionally, we have leaned on shaping the wavefront of the light beam, thereby utilizing various optical phenomena such as diffraction, reflection and phase accumulation in a medium. However, in the ever-evolving modern times, these techniques have been limited by their conventional laws of refraction/reflection, and the optical materials used are too bulky to be implemented in nano applications.

A metamaterial (MM) is a material that is specifically engineered and rarely found in naturally occurring materials. In other words, the source of its properties is not that of the material used but the custom-tailored structure. They are usually engineered in a repeating manner at sub-wavelength scales, i.e. at a scale which is smaller than the wavelengths of the phenomenon they influence. Metasurfaces (MS) are a 2-D manifestation of the same concept. They are usually single atomic layers thick and serve a similar purpose to metamaterials. Engineering of metasurfaces and metamaterials enabled us to harness the true potential of properties of light. Metamaterials have evolved into a breakthrough for controlling the electromagnetic properties on demand.

Metamaterials have always been held back by their challenges in bulk fabrication. This was overcome by the advent of metasurfaces, which evolved into a candidate to ma-

nipulate the wavefront, imitating optical devices at the nanoscale with compact design and subwavelength control[6]. Furthermore, metasurfaces have come into the limelight for their on-demand control over light beams' polarization, phase and amplitude. Initial attempts were made at metallic metasurfaces, which offered enhanced light-matter interaction but limited efficiency due to ohmic losses. Dielectric metasurfaces have overcome these issues and have paved a path for highly efficient and multi-functional meta-devices.

II. GENERAL BACKGROUND

In this section, we present some general concepts and background in Wave optics, which are required to understand the basics of light-matter interaction in the context of metasurfaces.

A. Polarization and Phases

In this subsection, we discuss Maxwell's equation, which leads to the plane wave solution and what the polarization of an EM wave refers to.

The four basic Maxwell's equations in free space are:

1. Gauss's Law for Electricity: $$\nabla \cdot \mathbf{E} = \frac{\rho}{\epsilon_0} \tag{1}$$
2. Gauss's Law for Magnetism: $$\nabla \cdot \mathbf{B} = 0 \tag{2}$$
3. Faraday's Law: $$\nabla \times \mathbf{E} = -\frac{\partial \mathbf{B}}{\partial t} \tag{3}$$
4. Ampère's Law (with Maxwell's correction): $$\nabla \times \mathbf{B} = \mu_0 \epsilon_0 \frac{\partial \mathbf{E}}{\partial t} \tag{4}$$

Here, $\mathbf{E}$ is the electric field, $\mathbf{B}$ is the magnetic field, ρ is the charge density, ϵ_0 is the permittivity of free space, and μ_0 is the permeability of free space.

Derivation of the Plane Wave Solution

Consider Maxwell's equations in free space where there are no charges ($\rho = 0$) and no currents ($\mathbf{J} = 0$).

From Faraday's Law (3):

$$\nabla \times \mathbf{E} = -\frac{\partial \mathbf{B}}{\partial t}.$$

From Ampère's Law (4):

$$\nabla \times \mathbf{B} = \mu_0 \epsilon_0 \frac{\partial \mathbf{E}}{\partial t}.$$

Taking the curl of Faraday's Law:

$$\nabla \times (\nabla \times \mathbf{E}) = -\frac{\partial}{\partial t}(\nabla \times \mathbf{B}).$$

Substituting Ampère's Law into the above:

$$\nabla \times (\nabla \times \mathbf{E}) = -\mu_0 \epsilon_0 \frac{\partial^2 \mathbf{E}}{\partial t^2}.$$

Using the vector identity:

$$\nabla \times (\nabla \times \mathbf{E}) = \nabla(\nabla \cdot \mathbf{E}) - \nabla^2 \mathbf{E},$$

and noting that $\nabla \cdot \mathbf{E} = 0$ in free space, this simplifies to:

$$-\nabla^2 \mathbf{E} = -\mu_0 \epsilon_0 \frac{\partial^2 \mathbf{E}}{\partial t^2}.$$

Thus, the wave equation for the electric field is:

$$\nabla^2 \mathbf{E} = \mu_0 \epsilon_0 \frac{\partial^2 \mathbf{E}}{\partial t^2}. \tag{5}$$

Plane Wave Solution

Assume a plane wave solution of the form:

$$\mathbf{E}(\mathbf{r}, t) = \mathbf{E}_0 e^{i(\omega t - \mathbf{k} \cdot \mathbf{r})}, \tag{6}$$

Where: - $\mathbf{E}_0$ is the amplitude, - $\mathbf{k}$ is the wave vector, - ω is the angular frequency, - $\mathbf{r}$ is the position vector, and - t is time.

Substitute back into the wave equation(5). The Laplacian of the plane wave is:

$$\nabla^2 \mathbf{E} = -|\mathbf{k}|^2 \mathbf{E}.$$

The second time derivative is:

$$\frac{\partial^2 \mathbf{E}}{\partial t^2} = -\omega^2 \mathbf{E}.$$

Equating these:

$$-|\mathbf{k}|^2 \mathbf{E} = -\mu\epsilon\omega^2 \mathbf{E}.$$

This gives the dispersion relation:

$$|\mathbf{k}|^2 = \mu\epsilon\omega^2.$$

Using $c^2 = \frac{1}{\mu_0 \epsilon_0}$, we find:

$$|\mathbf{k}| = n(r)\frac{\omega}{c} \tag{7}$$

Thus, the plane wave solution for $\mathbf{E}$ satisfies the wave equation and describes light propagation in free space.

In most applications, we consider the light beam propagating in the z direction; hence, the plane wave solution can be written as a matrix representation.

$$\vec{E} = \begin{bmatrix} E_{0x} e^{i(\omega t - kz + \phi_x)} \\ E_{0y} e^{i(\omega t - kz + \phi_y)} \end{bmatrix} = \begin{bmatrix} E_{0x} e^{i\phi_x} \\ E_{0y} e^{i\phi_y} \end{bmatrix} e^{i(\omega t - kz)} = \begin{bmatrix} E_{0x} e^{i(\phi_x - \phi_y)} \\ E_{0y} \end{bmatrix} e^{i(\omega t - kz + \phi_y)} \tag{8}$$

Looking at Eq(8), we can see that we just need the information of amplitude (E_{0x}, E_{0y}) and the phase difference $(\phi_x - \phi_y)$ to get complete information about a light beam upto a total phase. Polarization experiments usually take many cycles so that the overall global phase can be removed from the observation results.

1. Jones Algebra

Jones Vector

Following the motivation from the previous subsection, we build on the concept by defining a Jones vector:

$$\vec{E} = \begin{bmatrix} E_x \\ E_y \end{bmatrix} = \begin{bmatrix} E_{0x} \exp(-i\delta_x) \\ E_{0y} \exp(-i\delta_y) \end{bmatrix} \tag{9}$$

Polarization Type	**Jones Vector**
Horizontal (Linear)	$\begin{bmatrix} 1 \\ 0 \end{bmatrix}$
Vertical (Linear)	$\begin{bmatrix} 0 \\ 1 \end{bmatrix}$
45° Linear	$\frac{1}{\sqrt{2}} \begin{bmatrix} 1 \\ 1 \end{bmatrix}$
−45° Linear	$\frac{1}{\sqrt{2}} \begin{bmatrix} 1 \\ -1 \end{bmatrix}$
Right Circular (RCP)	$\frac{1}{\sqrt{2}} \begin{bmatrix} 1 \\ -i \end{bmatrix}$
Left Circular (LCP)	$\frac{1}{\sqrt{2}} \begin{bmatrix} 1 \\ i \end{bmatrix}$
General Elliptical	$\begin{bmatrix} a \\ be^{i\delta} \end{bmatrix}$

TABLE I: Jones Vectors for Common Polarization States

Coherency Matrix

The coherency matrix includes partial polarization effects by taking the temporal average of the direct product of the Jones vector by its Hermitian conjugate.

$$\phi = \langle E \otimes E^{\dagger} \rangle = \begin{bmatrix} \langle E_X E_X^* \rangle & \langle E_X E_Y^* \rangle \\ \langle E_Y E_X^* \rangle & \langle E_Y E_Y^* \rangle \end{bmatrix} = \begin{bmatrix} \phi_{xx} & \phi_{xy} \\ \phi_{yx} & \phi_{yy} \end{bmatrix} \tag{10}$$

2. Stokes-Mueller Algebra

Stokes Vector

We further build on the idea of the Stokes vector, which characterizes the electric field based on the intensities instead of the amplitudes since intensity is the measurable quantity in experiments. We define these measurable intensities in a 4x1 column vector representation called Stokes vector **S**:

$$\mathbf{S} = \begin{bmatrix} I \\ Q \\ U \\ V \end{bmatrix} = \begin{bmatrix} \langle E_x E_x^* \rangle + \langle E_y E_y^* \rangle \\ \langle E_x E_x^* \rangle - \langle E_y E_y^* \rangle \\ \langle E_x E_y^* \rangle + \langle E_y E_x^* \rangle \\ i(\langle E_x E_y^* \rangle - \langle E_y E_x^* \rangle) \end{bmatrix} = \begin{bmatrix} I_H + I_V \\ I_H - I_V \\ I_P + I_M \\ I_R - I_L \end{bmatrix} \tag{11}$$

where I is the total detected light intensity that corresponds to the addition of the two orthogonal component intensities; Q is the difference in intensity between horizontal and vertical polarization states; U is the difference between the intensities of linear 45° and +45°(135°) polarization states; and V is the difference between intensities of right circular and left circular polarization states. Thus, these parameters can be directly determined by the following six intensity measurements (I) performed with ideal polarizers: I_H, horizontal linear polarizer (0°); I_V, vertical linear polarizer (90°); I_P, 45° linear polarizer; I_M 135°(−45°) linear polarizer; I_R, right circular polarizer, and I_L, left circular polarizer.

State	H	V	P	M	R	L	Elliptical
S	$\begin{bmatrix} 1 \\ 1 \\ 0 \\ 0 \end{bmatrix}$	$\begin{bmatrix} 1 \\ -1 \\ 0 \\ 0 \end{bmatrix}$	$\begin{bmatrix} 1 \\ 0 \\ 1 \\ 0 \end{bmatrix}$	$\begin{bmatrix} 1 \\ 0 \\ -1 \\ 0 \end{bmatrix}$	$\begin{bmatrix} 1 \\ 0 \\ 0 \\ 1 \end{bmatrix}$	$\begin{bmatrix} 1 \\ 0 \\ 0 \\ -1 \end{bmatrix}$	$\begin{bmatrix} 1 \\ cos2\alpha cos2\epsilon \\ sin2\alpha cos2\epsilon \\ -sin2\epsilon \end{bmatrix}$

TABLE II: Normalized Stokes Vector for Common Polarization States

Mueller Matrix

The Jones vector representation can be converted to the Stokes vector representation using the Mueller matrix transformation. Firstly, we can see that the relation between the Stokes vector and the coherency vector can be easily given by:

$$S = \begin{bmatrix} \phi_{xx} + \phi_{yy} \\ \phi_{xx} - \phi_{yy} \\ \phi_{xy} + \phi_{yx} \\ i(\phi_{yx} - \phi_{xy}) \end{bmatrix}$$

Therefore, we can transform any coherency vector to a stokes vector by the following

transformation:

$$S = A \begin{bmatrix} \phi_{xx} \\ \phi_{xy} \\ \phi_{yx} \\ \phi_{yy} \end{bmatrix}, A = \begin{bmatrix} 1 & 0 & 0 & 1 \\ 1 & 0 & 0 & -1 \\ 0 & 1 & 1 & 0 \\ 0 & -i & i & 0 \end{bmatrix} \tag{12}$$

Finally, Mueller matrices are defined to show the transformation of polarization of incident light after a medium.

$$S_0 = MS_i \tag{13}$$

where S_0 and S_i are the output and input stokes vectors, respectively.

To obtain the relationship between Mueller and Jones matrix, we first consider how the Jones matrix transforms the coherency matrix.

$$C_i = E_i E_i^\dagger; E_o = JE_i; C_0 = E_0 E_0^\dagger$$

$$\therefore C_0 = (JE_i)(JE_i)^\dagger = JE_i E_i^\dagger J^\dagger = JC_i J^\dagger \tag{14}$$

Next, we use the property of vectorization, which connects the matrix multiplication with the Kroneckar product:

$$vec(ABC) = (C^T \otimes A)vec(B) \tag{15}$$

where $A \otimes B = \begin{bmatrix} a_{11}B & a_{12}B \\ a_{21}B & a_{22}B \end{bmatrix}$ is defined as the kroneckar product and $vec(A) = \begin{bmatrix} a_{11} \\ a_{12} \\ a_{21} \\ a_{22} \end{bmatrix}$.

Applying this to Eq(14):

$$vec(C_0) = vec(JC_i J^\dagger) = ((J^\dagger)^T \otimes J)vec(C_i)$$

$$\therefore L_0 = (J^* \otimes J)L_i \tag{16}$$

Finally, we can now express the Mueller matrix:

$$\begin{gathered} S_0 = MS_i \\ S_0 = AL_0 = A(J^* \otimes J)L_i \\ \because S_i = AL_i \implies S_0 = A(J^* \otimes J)A^{-1}S_i \end{gathered} \tag{17}$$

Hence, we get the expression for the Mueller matrix as follows:

$$M = A(J^* \otimes J)A^{-1} = A(J \otimes J^*)A^{-1} \tag{18}$$

3. *Poincaré Sphere*

The Poincaré sphere is an excellent geometrical representation of all polarizable states. Totally polarizable states are given by the points on the sphere's surface, while the partially polarized points are inside the sphere. In this geometric representation, the points on the equator represent the linearly polarized state, while the north and south poles represent the right and left circularly polarized light, respectively. In further sections, we will see how we can use this representation to calculate geometric phases effectively.

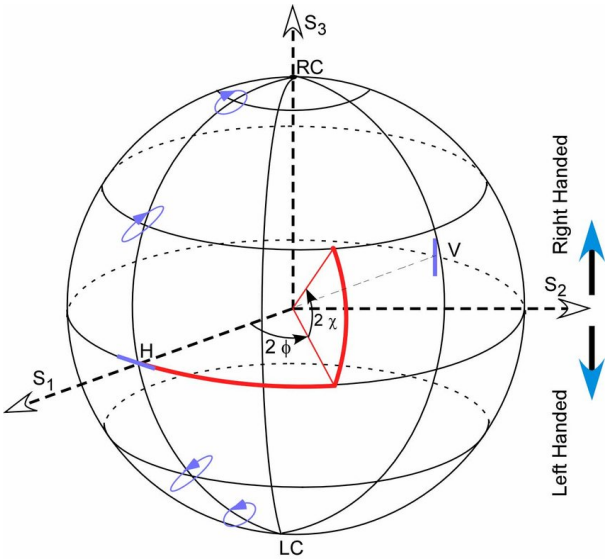

FIG. 1: *Poincaré Sphere representation of Stokes Vector*

4. *Optical Devices*

In this subsection we will see how various optical devices can be represented mathematically in the Jones Matrix formalism. This helps us to calculate the output of these optical devices easily.

- Linear Polarizer: It lets light transmit at any arbitrary angle θ and blocks/emits

the orthogonal components:

$$P_\theta = \begin{bmatrix} cos^2\theta & cos\theta sin\theta \\ cos\theta sin\theta & sin^2\theta \end{bmatrix} \tag{19}$$

- Linear Retarder: A linear retarder introduces a phase difference (δ) between the two orthogonal polarization components.
  - General Linear Retarder:
    $$R = \begin{bmatrix} e^{i\phi_x} & 0 \\ 0 & e^{i\phi_y} \end{bmatrix} \tag{20}$$
    where $\delta = \phi_x - \phi_y$ is the phase retardation.
  - Quarter Wave Plate (QWP): $\delta = \pi/2$
    $$QWP = \begin{bmatrix} 1 & 0 \\ 0 & i \end{bmatrix} \tag{21}$$
  - Half Wave Plate (HWP): $\delta = \pi$
    $$HWP = \begin{bmatrix} 1 & 0 \\ 0 & -1 \end{bmatrix} \tag{22}$$
  - At arbitrary θ:
    $$R_\theta = \begin{bmatrix} e^{i\phi_x}cos^2\theta + e^{i\phi_y}sin^2\theta & (e^{i\phi_x} - e^{i\phi_y})cos\theta sin\theta \\ (e^{i\phi_x} - e^{i\phi_y})cos\theta sin\theta & e^{i\phi_x}sin^2\theta + e^{i\phi_y}cos^2\theta \end{bmatrix} \tag{23}$$
  - Spiral Wave Plate (SWP): It generates optical vortex beams with orbital angular momentum(Sec II B 1). To represent it in Jones formalism, it includes the dependence on azimuthal angle.
    $$SWP(\phi) = \begin{bmatrix} e^{il\phi} & 0 \\ 0 & e^{-il\phi} \end{bmatrix} \tag{24}$$
    where l is the topological charge.

- Rotator: It rotates the polarization of light by an angle θ

$$R(\theta) = \begin{bmatrix} cos\theta & sin\theta \\ -sin\theta & cos\theta \end{bmatrix} \tag{25}$$

- Circular Polarizer: It converts linearly polarized light into circularly polarized light or vice-versa. It can be understood as a combination of linear polarizer and QWP.
  - Right Circular Polarizer:

$$C_R = \frac{1}{2} \begin{bmatrix} 1 & i \\ -i & 1 \end{bmatrix} \tag{26}$$

  - Left Circular Polarizer:

$$L_R = \frac{1}{2} \begin{bmatrix} 1 & -i \\ i & 1 \end{bmatrix} \tag{27}$$

Using Eq(18), we can convert these fundamental Jones matrices to Mueller matrices, which is a 4x4 matrix containing all information about how a medium affects the polarization of input light beam and can be regarded as the complete optical polarization fingerprint of a sample.

Furthermore, any of these optical instruments can be rotated by an angle θ by using the following similarity transformation:

$$J^{'} = R^{-1}(\theta)JR(\theta) \ \& \ M^{'} = T^{-1}(\theta)MT(\theta) \tag{28}$$

where R is the rotation matrix and $T(\theta)$ is given by:

$$T(\theta) = \begin{bmatrix} 1 & 0 & 0 & 0 \\ 0 & cos2\theta & sin2\theta & 0 \\ 0 & -sin2\theta & cos2\theta & 0 \\ 0 & 0 & 0 & 1 \end{bmatrix}$$

B. Angular Momentum of Light

This section discusses the various types of angular momentum carried by light. A paraxial optical beam of light can carry three types of angular momentum: spin angular momentum (SAM), orbital angular momentum (OAM) and extrinsic orbital angular

momentum (EOAM).

We begin by defining the linear momentum density and the angular momentum densities of the EM wave in terms of E and B[7]:

$$p = \epsilon_0 E \times B; j = r \times p = \epsilon_o r \times (E \times B) \tag{29}$$

Therefore, the total densities can be found by integrating them:

$$P = \int \epsilon_0 (E \times B) \cdot dr; J = \int \epsilon_0 r \times (E \times B) \cdot dr \tag{30}$$

We are now attempting to separate the SAM and OAM. It is essential to understand that if we consider the ideal case, i.e. a plane wave travelling in purely z direction, then the direction of $E \times B$ is the same as r or the direction of propagation. It is necessary to grasp that such a plane wave is an idealized concept and cannot exist in reality.

Real optical beams are limited in spatial extent either by the beams themselves or by the finite extent of the measurement system used to detect them, and this leads to a nonzero longitudinal component of the field. This longitudinal component of the field arises from the radial gradient of the field that occurs at the edge of the beam or the measurement system, which eventually leads to a value of angular momentum of $\pm\hbar$ per photon (for left/right circular polarization) when integrated over the cross-section of the entire beam.

We invoke paraxial approximation for the light beam, which dictates that the transverse dimensions are much smaller than the longitudinal distance over which the fields change their magnitude. Under paraxial approximation, we generally write the electric field as[8]:

$$E(x, y, z) = F(x, y, z)e^{ikz} \tag{31}$$

where F(x,y,z) is the slowly changing parameter and under paraxial approximation, it is assumed that the derivative of F with respect to z is negligible compared to transverse derivatives. It can be expressed as:

$$2ik\frac{\partial}{\partial z}F = -\left(\frac{\partial^2}{\partial x^2} + \frac{\partial^2}{\partial y^2}\right) \tag{32}$$

Using Maxwell's law(3) and (1) in the context of paraxial approximation and performing algebraic manipulations, we can write the z component of the angular momentum as:

$$
\begin{aligned}
j_z(x,y,z) &= \left[\frac{\omega\epsilon_0}{2i}E^*(\hat{r}\times\nabla)E\right]_z + \left[\frac{\omega\epsilon_0}{2i}E^*\times E\right]_z \\
&= \frac{\omega\epsilon_0}{2i}\left[F_k^*\left(x\frac{\partial}{\partial y}-y\frac{\partial}{\partial x}\right)F_k\right]_{k=x,y} + \frac{\omega\epsilon_0}{2i}(F_x^*F_y - F_y^*F_x)
\end{aligned}
\tag{33}
$$

Looking at Eq(33), we can see that the first term carries the transverse distribution of the EM wave, i.e. amplitude and phase. In contrast, the second term contains information about the polarization and is proportional to the fourth element of the Stokes vector described in Eq(11). Hence, we conclude that the first term corresponds to OAM and the second to the SAM. For optical vortex beams explained in sectionII B 1, we can express the transverse field as:

$$
F(r,\phi) = u(r)\exp(il\phi)\hat{F} \tag{34}
$$

where we know that $x\frac{\partial}{\partial y} - y\frac{\partial}{\partial x} = \frac{\partial}{\partial \phi}$ for cylindrical symmetric system and we define the normalized quantity, $i(F_x^*F_y - F_y^*F_x) = \sigma \in [-1,1]$ as the wave helicity.

$$
j_z(r,\phi) = (\sigma + l)\epsilon_0\omega^2|u(r)|^2 \tag{35}
$$

We can also write the energy density of the paraxial beam as:

$$
w = c\epsilon_0(E\times B)_z = c\omega k\epsilon_0|u(r)|^2 = \epsilon_0\omega^2|u(r)|^2 \tag{36}
$$

Using Eq(35) and Eq(36), we can write the ratio of angular momentum to energy density as:

$$
\frac{j_z}{w} = \frac{\sigma + l}{w} \tag{37}
$$

It should be observed that spin, σ, is said to be intrinsic because it is independent of the choice of the axis about which it is calculated. However, orbital, l, depends upon the choice of axis. Nevertheless, when there is a direction, z, for which the transverse linear momentum of the beam is zero, both l and σ are invariant under a shift of axis, and the orbital component might be said to be quasi-intrinsic[9].

1. Intrinsic Angular Momentum

Spin Angular Momentum

SAM is produced by rotating electric and magnetic fields in circularly polarized light beams. The spin angular momentum is aligned along the direction of propagation or the

z-axis. It depends on the light's polarization helicity, i.e. $\sigma \in (-1, 1)$. The helicity is +1 for right circularly polarized light and -1 for left.

$$S = \sigma \hat{p} \tag{38}$$

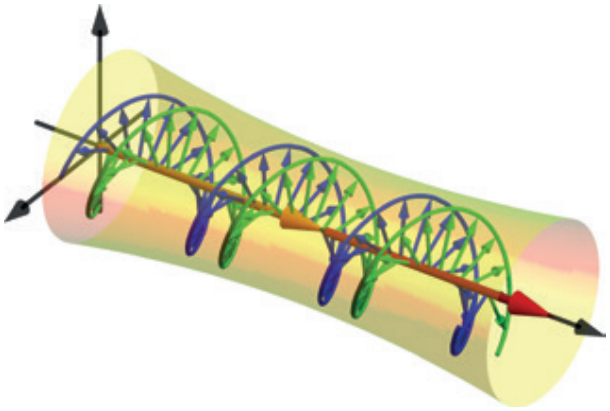

FIG. 2: *SAM for a right-handed circularly polarized light with $\sigma = 1$[1]*

SAM can be measured experimentally using polarization techniques and Stokes parameters. We can use a series of wave plates and then measure the final Stokes vector to get information about the input light beam. We define the canonical SAM density as [10]:

$$S = \frac{g}{2} Im[\epsilon E^* \times E + \mu H^* \times H] \tag{39}$$

Orbital Angular Momentum

Optical vortex beams carry orbital angular momentum. Optical vortex beams are the ones with a doughnut-like intensity profile along with an azimuthal phase dependence called the Hilbert factor ($\exp(il\theta)$) with respect to the beam axis, which is the helicoidally shaped wavefront. The number of twists (l) of the wavefront within a wavelength is called the topological charge of the vortex beam. It is related to L by $L = \hbar l$ where $\hbar$ is the Planck constant. These vortex beams are usually generated by spiral waveplates.

$$L^{int} = l\hat{p} \tag{40}$$

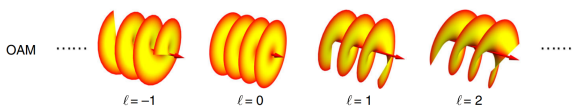

FIG. 3: *Phase distribution for various eigenstates of OAM[2]*

OAM of light can be measured using interferometric methods i.e. by interfering it with a reference gaussian beam and observing the resultant inferference pattern, we can analyze the topological charge l of the vortex beam containing OAM.

2. Extrinsic Angular Momentum

Finally, extrinsic AM is carried by a light beam propagating at some distance from the coordinate origin. This angular momentum is analogous to the classical AM given by the cross-product of the transverse position of the beam centre and its momentum. Say the axis is displaced by some $r_0 = (r_{0x}, r_{oy})$, then we define the change the angular momentum as:

$$\Delta J_z = (r_{ox} \times P_y) + (r_{0y} \times P_x) = r_{ox}\epsilon_0 \int (E \times B)_y dxdy + r_{0y}\epsilon_0 \int (E \times B)_x dxdy \quad (41)$$

We call OAM as extrinsic if $\Delta J_z = 0$ for all values of (r_{ox}, r_{oy})(EOAM=0 for cylindrically symmetic vortex beams) or in other words:

$$\int (E \times B)_y dxdy = 0 \ \& \int (E \times B)_x dxdy = 0 \quad (42)$$

$$L^{ext} = R \times P \quad (43)$$

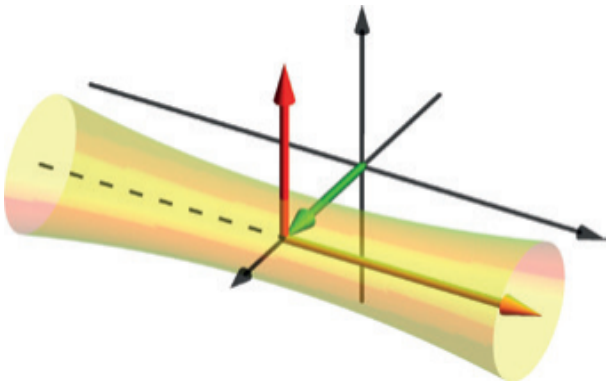

FIG. 4: *EOAM due to propagation of light beam at a distance R from the coordinate origin[1]*

C. Geometric Phase

The light beam carries two major phases during propagation. The phase associated with the optical path is defined as the dynamical phase and is given by:

$$\Theta_d = \frac{2\pi}{\lambda} \times \textit{optical path} \tag{44}$$

where λ is the wavelength of the light. The dynamical phase is responsible for most interference patterns. The geometric phase is independent of the light path and is based only on the geometry, as the name suggests, or on the evolution of the light wave. The geometric phase plays a significant role when light interacts with inhomogeneous isotropic/non-isotropic mediums; hence, it is crucial to understand this concept to know about its interaction with metasurfaces. Geometric phases are broadly divided into two categories, named the spin redirection Berry phase and the Pancharatnam-Berry (PB) phase.

1. Spin redirection Berry phase

This geometrical phase arises from the adiabatic evolution of the wave vector k in a curved trajectory, for instance, in an optical fibre cable, as shown in Figure 5. The condition for adiabatic evolution is: i) The helicity of the wave shouldn't change locally as the wave propagates. ii) Medium shouldn't have any birefringement(anisotropy). That is, there should not be a local change in the polarization of light as it propagates.

We will try to obtain a mathematical expression for spin redirection Berry phase by analyzing the phase in the momentum space where θ and ϕ are angles subtended by wave vector on the k_z and k_x axis, respectively. We write it in polar coordinates as follows from the lab frame:

$$(k_x, k_y, k_z) = k(\sin\theta\cos\phi, \sin\theta\sin\phi, \cos\theta) \tag{45}$$

As we can observe, the orientation of polarization ($\vec{e}$) changes by Θ in the lab frame but remains constant in the frame of the light. This phase shift can be calculated by calculating the area of the shaded region in the k-sphere in Figure 5, which is equal to

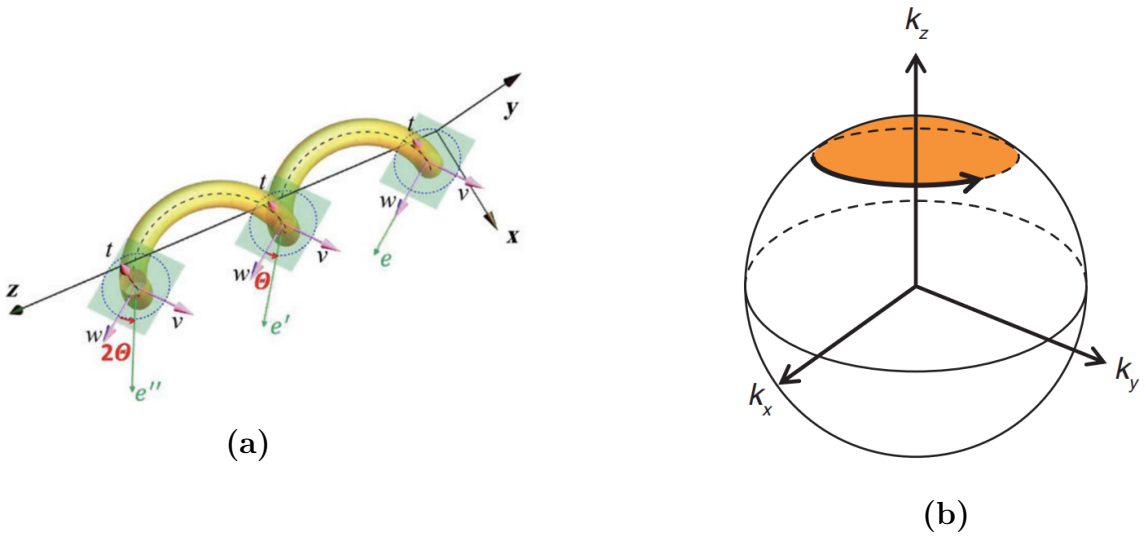

(a) **(b)**

FIG. 5: *(a) Polarization ($\vec{e}$) evolving in a helical trajectory along with coordinates marked in the reference frame of propagation of light(v,w,t).[3] (b) Representation of one full cyclic evolution in the momentum space[4]*

the solid angle subtended by the trajectory.

$$\Theta = \int_0^{\theta} \sin\theta d\theta \int_0^{2\pi} d\phi = 2\pi(1-\cos\theta) \tag{46}$$

To see how a linearly polarized light obtains this geometric phase, we consider a linearly polarized light beam along the x-axis in terms of left circularly polarized light and right circularly polarized light:

$$|x\rangle = \frac{1}{\sqrt{2}}(|L\rangle + |R\rangle)$$

After one full cycle, the polarisation can now be written as the left circularly polarized light obtains a phase of Θ and the right circularly polarized light obtains $-\Theta$.

$$|x_{out}\rangle = \frac{1}{\sqrt{2}}\left(e^{i\Theta}|L\rangle + e^{-i\Theta}|R\rangle\right) \tag{47}$$

Therefore, to measure this phase experimentally, we measure the intensity after N turns in the optical cable in a detector. The phase after N turns from Eq(46) will be equal to $\Theta = \pm 2\pi N(1-\cos\theta)$ for LCP and RCP respectively. Therefore, the resultant intensity detected in the detector can be written as:

$$I = I_0 \cos^2[2\pi N(1-\cos\theta)] \tag{48}$$

Hence, the final intensity depends on the pitch angle of the helix (θ) and the number of turns(N).

2. Pancharatnam-Berry phase

The PB phase arises when a light beam changes its polarization continuously while keeping the direction of propagation fixed. Such a phase is acquired when polarized light travels through an anisotropic medium, which changes its phase. To calculate this phase, we define a complex scalar product called the Pancharatnam connection, which is a connection between two distant states on a Poincaré sphere and is given by the phase difference between two states $|A\rangle$ and $|B\rangle$ as $arg(\langle A|B\rangle)$.

Based on Pancharatnam's theory of interference, we consider an example and calculate the phase difference between 2 light beams. The following transformations are done on an initially linearly polarized light beam:

- Case 1 (Red Path in Fig(6)): Horizontally polarized light is passed through a QWP at 45° which makes it RCP and then through a rotated linear polarizer which makes it rotated by some angle ϕ.
- Case 2 (Blue Path in Fig(6)): Horizontally polarized light is passed through a QWP at $-45°$ which makes it LCP and then through a rotated linear polarizer which makes it rotated by some angle ϕ.

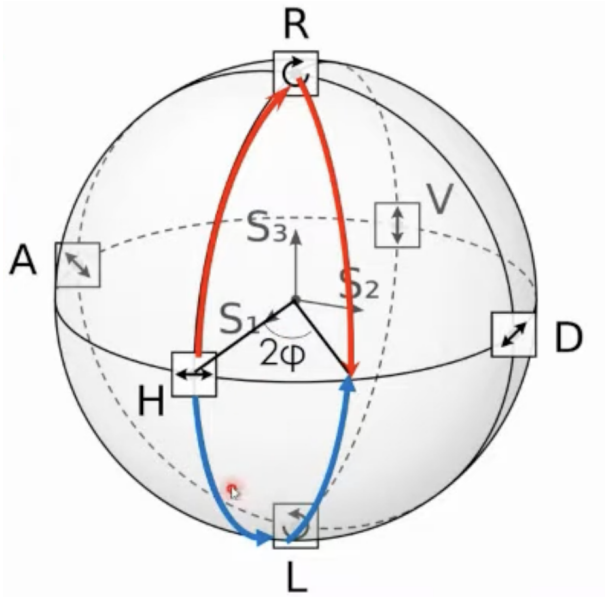

FIG. 6: *A linearly polarized light undergoes transformation through two different paths represented by red and blue and acquires a phase difference of* 2ϕ

We can calculate this phase difference by writing the Jones matrices given in section II A 4 for the respective transformations, which comes out to be half of the enclosed area shown in Fig(6).

III. THEORETICAL AND MATHEMATICAL BACKGROUND

In this section, we build a theoretical framework based on our understanding from section II. We can proceed by understanding the interaction of metasurfaces with EM waves. At its core, metasurfaces are nothing but imitating the optical devices as discussed in section II A 4 in a 2-D and wavelength scale. We aim to custom-tailorize the light's wavefront so that our 2-D metasurface can alter different properties of light(Amplitude, polarization, phase, SAM, OAM) based on our needs. We shall proceed by first understanding a generalized Snell's law for metasurfaces, which will serve as a guiding basis for how light reflects and refracts when it encounters a metasurface thereby understanding how metasurfaces are imitating optical instruments by a gradient in phase discontinuity.

A. Generalized Snell's Law

Generalized Snell's law dictates how metamaterials and metasurfaces bend light and provides us with a new degree of freedom by introducing a phase discontinuity in the medium at a wavelength scale. We invoke Fermat's principle to prove the generalized law of reflection and refraction. It is pretty analogous to the least action principle, which states that light travelling in any medium from A to B takes the least optical path. We state it in a similar mathematical fashion to the least action principle that the derivative of the phase accumulated ($\int_A^B d\phi(\vec{r})$) along a light path will be zero with respect to infinitesimal variations of the path. Therefore, the total phase difference for a light beam will be given by:

$$\phi_{tot}(\vec{r}) = \Phi(\vec{r_s}) + \int_A^B \vec{k} \cdot d\vec{r} \tag{49}$$

where $\vec{r_s}$ is the vector along the surface interface, Φ is the abrupt discontinuity of phase, and the second term is the usual phase difference from the optical path. We can write

the generalized formula as follows:

$$\begin{aligned} k_{r,x} &= k_{i,x} + \frac{\partial \phi}{\partial x} \\ k_{t,x} &= k_{i,x} + \frac{\partial \phi}{\partial x} \end{aligned} \tag{50}$$

Where $k_{i,x}, k_{r,x}$ and $k_{t,x}$ are the x-components of the wavevectors of the incident, reflected and transmitted light, respectively. At the same time, $\partial\phi/\partial x$ is the phase gradient. Consider an incident plane wave as shown in Fig(7) at an angle of θ_i, we use Eq(49) and state that the phase difference between two paths infinitesimally close to each other must be zero which gives us:

$$[k_0 n_i \sin(\theta_i) dx + (\Phi + d\Phi)] - [k_0 n_t \sin(\theta_t) dx + \Phi] = 0 \tag{51}$$

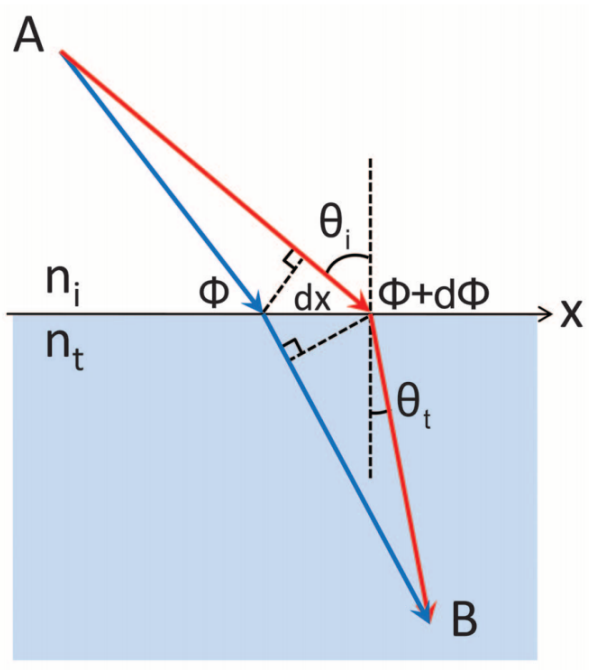

FIG. 7: *The surface interface between the medium is structured to introduce abrupt phase discontinuity in the light path[5]*

Here $k_0 = \frac{2\pi}{\lambda_0}$ where λ_0 is the wavelength of light in vacuum. This gives us the generalized Snell's law as:

$$\sin(\theta_t) n_t - \sin(\theta_i) n_i = \frac{\lambda_0}{2\pi} \frac{d\Phi}{dx} \tag{52}$$

Observing Eq(52), we can see that we can achieve any arbitrary value of θ_t if we set our

value for $\frac{d\Phi}{dx}$ appropriately. Since we have different values of θ_t for $\pm\theta_i$, we will have two different critical angles in the case of generalized Snell's law. We can easily calculate critical angle now:

$$\theta_c = \arcsin\left(\pm\frac{n_t}{n_i} - \frac{\lambda_0}{2\pi n_i}\frac{d\Phi}{dx}\right) \tag{53}$$

Subsequently, we can write the generalized law for reflection too:

$$\sin(\theta_r) - \sin(\theta_i) = \frac{\lambda_0}{2\pi n_i}\frac{d\Phi}{dx} \tag{54}$$

Where θ_r is the angle of reflection. We get a non-linear connection between the angle of reflection and the angle of incident, which indicates that there is always a critical angle of incident, beyond which the reflected beam will become evanescent or die out really fast. This critical angle of incidence is given by:

$$\theta_c^{'} = \arcsin\left(1 - \frac{\lambda_0}{2\pi n_i}\left|\frac{d\Phi}{dx}\right|\right) \tag{55}$$

B. Spin Hall Effect

We saw in the previous section how a change in the trajectory of a light beam induces a phase difference. In the context of optics in metasurfaces, the optical spin hall effect (OSHE) refers to the change in the trajectory of the wavefront of light based on spin splitting, i.e. the two spins referring to LCP and RCP components of the light beam—such a change in trajectory results from a sharp change in the refractive index of the metasurface.

1. Berry connection and Berry curvature

Consider an LCP light beam whose polarization can be depicted by $\psi = (\hat{\theta} + i\hat{\phi})/\sqrt{2}$ where $(\hat{k}, \hat{\theta}, \hat{\phi})$ is the standard circular polar coordinates with $\hat{k}$ as the wave vector. The berry connection can be calculated easily by $A = i\langle\psi|\nabla_r|\psi\rangle$. Before proceeding, we note

these results from polar coordinates which will be used:

$$\begin{aligned}\frac{\partial\hat{r}}{\partial\theta}=\hat{\theta};\frac{\partial\hat{r}}{\partial\phi}=\sin\theta\hat{\phi}\\ \frac{\partial\hat{\theta}}{\partial\theta}=-\hat{r};\frac{\partial\hat{\theta}}{\partial\phi}=\cos\theta\hat{\phi}\\ \frac{\partial\hat{\phi}}{\partial\theta}=0;\frac{\partial\hat{\phi}}{\partial\phi}=-\sin\theta\hat{r}-\cos\theta\hat{\theta}\end{aligned} \tag{56}$$

Now we calculate the A_θ component for berry connection:

$$A_\theta=i\left\langle\psi\middle|\frac{\partial}{\partial\theta}\middle|\psi\right\rangle=i\left(\frac{1}{\sqrt{2}}\left(\hat{\theta}-i\hat{\phi}\right)\cdot\left(\frac{1}{\sqrt{2}}\frac{\partial\hat{\theta}}{\partial\theta}\right)\right)=0 \tag{57}$$

by noting that, $\because\hat{\theta}\cdot\frac{\partial\hat{\theta}}{\partial\theta}=0$. Next, we similarly calculate A_ϕ:

$$\begin{aligned}A_\phi=i\left\langle\psi\middle|\frac{\partial}{\partial\phi}\middle|\psi\right\rangle&=i\left(\frac{1}{\sqrt{2}}\left(\hat{\theta}-i\hat{\phi}\right)\cdot\left(\frac{1}{\sqrt{2}}\left(\cos\theta\hat{\phi}-i\cos\theta\hat{\theta}\right)\right)\right)\\ &=\frac{i}{2}\left(-i\cos\theta-i\cos\theta\right)=\cos\theta\end{aligned} \tag{58}$$

Next, we calculate the berry curvature using the formula for berry curvature:

$$\Omega=\partial_\theta A_\phi-\partial_\phi A_\theta=-\sin\theta \tag{59}$$

The corresponding geometric phase is easy to calculate by integrating the Berry curvature, which is nothing but the area of the This Berry connection A(k) acts like a vector potential in the momentum space, and Berry curvature is nothing but the curl of this vector potential, i.e. $\Omega=\nabla\times A$. This motivates us to see the Berry curvature as an analogous effective magnetic field that behaves like a magnetic monopole at the k-space's origin.

2. Equations of motion

Having laid out the mathematical foundations, we now attempt to mathematically calculate the equations of motion of photons in an isotropic, smoothly inhomogeneous medium by adopting a semi-classical approach. We begin by citing the results given by Berry's work[11] where it is stated that in adiabatic approximation, we can write a field

tensor or, in our case, the Berry curvature in the following manner:

$$F_{ij} = m\epsilon_{ijk}\frac{g_k}{g^3}; \Omega = m\frac{\mathbf{g}}{g^3} \tag{60}$$

where $\mathbf{g}$ stands for 3-D space where photon transport is considered and m stands for the projection of particle's spin and $m = \pm 1$ for RCP and LCP photons respectively. Additionally, we also describe some of the general statements to start geometric optics:

$$\mathbf{p} = k_0^{-1}\mathbf{k}; \omega = \pm kc \tag{61}$$

where k stands for wavevector, k_0 is the central wavenumber and p is the dimensionless wave momentum. We start by defining the Hamiltonian for a photon in the medium[12]:

$$H(p, r) = \frac{1}{2}\left(|p|^2 - n^2(r)\right) \tag{62}$$

where p is the momentum of the photon, $n(r)$ is the refractive index at position r. We introduce the Berry connection or the vector potential A due to the photon's polarization in the momentum space. The modified Hamiltonian incorporating this Berry connection is given by Eq(63)

$$H(p, R) = \frac{1}{2}\left(|p|^2 - n^2\left(R - \frac{1}{k_0}A(p)\right)\right) \tag{63}$$

Here, R is the generalized coordinates to p and the physical coordinate r is related to R by Eq(64)

$$r = R - \frac{1}{k_0}A(p) \tag{64}$$

Next, we consider the Taylor expansion of refractive index term $n^2\left(R - \frac{1}{k_0}A(p)\right)$ around R up to order $O(k_0^{-1})$:

$$n^2\left(R - \frac{1}{k_0}A(p)\right) \approx n^2(R) - \frac{1}{k_0}(A(p) \cdot \nabla_R n^2(R)) + O(k_0^{-2}) \tag{65}$$

Substituting it back into Eq(63),

$$H(p, R) = \frac{1}{2}\left(|p|^2 - n^2(R) + \frac{1}{k_0}(A(p) \cdot \nabla_R n^2(R))\right) \tag{66}$$

We know that Hamilton's equation in generalized p and R are:

$$\dot{p} = -\nabla_R H; \dot{R} = \nabla_p H \tag{67}$$

We compute the gradient of H with respect to R:

$$\nabla_R H = \frac{1}{2}\left(-\nabla_R n^2(R) + \frac{1}{k_0}\nabla_R(A(p)\cdot\nabla_R n^2(R))\right) \tag{68}$$

However, we know that $A(p)$ only depends on p and the term $\nabla_R A(p) = 0$. Using $n^2(r) \approx n^2(R)$ since R and r differ by a term of order $O(k_0^{-1})$. Hence, up to order $O(k_0^{-1})$:

$$\dot{p} = \frac{1}{2}\nabla_r n^2(r) \tag{69}$$

Similarly, we write the equation for generalized position coordinates by computing the gradient of H with respect to p:

$$\nabla_p H = p + \frac{1}{k_0}\nabla_p(A(p)\cdot\nabla_R n^2(R)) \tag{70}$$

Simplifying the second term in the above equation, we can again say that the term involving $\nabla_p A(p)$ is of order $O(k_0^{-1})$ and hence, can be neglected:

$$\dot{R} = \nabla_p H = p \tag{71}$$

Recalling Eq(64), we differentiate it w.r.t time and substitute the result of Eq(71):

$$\dot{r} = p - \frac{1}{k_0}\left(\frac{\partial A}{\partial p}\cdot\dot{p}\right) \tag{72}$$

We now introduce our definition for Berry curvature, which was $\Omega = \nabla_p \times A(p)$. We introduce an identity, which can be proved by using simple vector arithmetic:

$$\left(\frac{\partial A}{\partial p}\cdot\dot{p}\right) = \Omega(p)\times\dot{p} \tag{73}$$

Therefore, the Eq(72) becomes:

$$\dot{r} = p - \frac{1}{k_0}\left(\Omega(p)\times\dot{p}\right) \tag{74}$$

Finally, after all the maths, we can write down the equations for motion. From Eq(69), we write the momentum equation by dividing by $n(r)$ on both sides:

$$\frac{1}{n(r)}\dot{p} = \frac{1}{2n(r)}\nabla_r n^2(r) = \nabla_r n(r) \tag{75}$$

Since, $p = n(r)k$, we conclude at:

$$\frac{\partial k}{\partial t} = \nabla_r n(k); \dot{p} = n(r)\frac{\partial n}{\partial r} \tag{76}$$

Similarly, now for the position, continuing from Eq(74), we substitute Berry's result Eq(60) and write:

$$\dot{r} = p \mp \frac{1}{k_0}\left(\frac{p}{|p|^3} \times \dot{p}\right) \tag{77}$$

C. Physical Interpretation

The following equations, Eq(77) and Eq(76) represent the propagation trajectory of EM waves in the first approximation of geometric optics. The second term of Eq(77) represents the Magnus optical effect or the topological spin transport of photons. It can also be thought of as a consequence of the anomalous Hall effect of photons. Hence, this causes a split in the trajectory due to spins, which we call spin split due to the gauge potential (Berry connection) and a field (Berry curvature). As one can guess, we can indeed calculate the magnitude of splitting for RCP and LCP by a contour integral in the momentum space for the last term of Eq(77). We get:

$$\delta r = \mp k_0^{-1}\int_0^s \frac{(p \times \dot{p})}{p^3} ds = \mp k_0^{-1}\int_L \frac{p \times dp}{p^3} \tag{78}$$

where L is the contour in the p-space along which the photon moves. We concur that the Magnus effect is a topological nonlocal effect, similar to the Berry phase. We can further go ahead and calculate the general phase, given by Eq(49):

$$\begin{aligned} \phi &= -\omega t + k_0 \int_0^S p dR \\ &= -\omega t + k_0 \int_0^S p dr - \int_L A dp \end{aligned} \tag{79}$$

The first and second terms in Eq(79) represent the usual dynamic and geometric phase, respectively. In contrast, the third term is the geometric Berry phase, given by contour integral in the momentum space. We can now also describe the group velocity and phase velocity:

$$v_g = \frac{d\omega}{dk} \equiv -\frac{\partial H/\partial k}{\partial H/\partial \omega} = \frac{c}{n^2}\dot{r} = \frac{c}{n}\left[1 \mp k_0^{-1}\frac{(p \times \dot{p})}{p^3}\right] \tag{80}$$

$$v_{ph} = \frac{\omega}{|k|} \equiv \frac{\partial \phi/\partial t}{|\partial \phi/\partial r|^2}\frac{\partial \phi}{\partial r} = \frac{c}{n}\frac{\mathbf{p}}{p}\left[1 + k_0^{-1}\frac{A\dot{\mathbf{p}}}{p}\right] \tag{81}$$

IV. EXPERIMENTAL DISCUSSIONS

We now move on from our mathematical framework and use its results to show its implications in experimental domains. Based on the interaction of light with metasurfaces, we can divide the metasurfaces broadly into the following categories.

A. Multi Resonance Metasurface

Multi-resonance MS is the simplest form of MS and was the first one to be developed in the field. The equations of motions derived in Section III B 2 were interpreted and used to develop these. Using the equation of motions, we could see that different k-components of the wavefront evolve with a different additional spin-dependent geometric phase, which led to a beam splitting as shown in Fig(8).

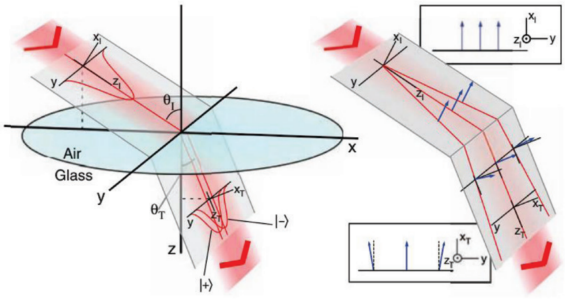

FIG. 8: *Spin-splitting of light due to spin-dependent geometric phase picked up by different k-components[4]*

V-shaped antennas comprising two nanorods (Fig(9)) of equal lengths joined at some arbitrary angle were the first proposed design for the nanostructure of MS, which offered a complete phase variation of 0 to 2π. These V-shaped antennas offer two resonant modes, symmetric and anti-symmetric, which correspond to the excitation of modes when

the incident light is parallel or perpendicular to the symmetry axis, respectively. This splitting respects the time-reversal symmetry but violates the inversion symmetry, which also manifests in OSHE. This linear gradient of the transmission phase profile bends the light beam, and this bending angle can be achieved arbitrarily by changing the shape of the metasurface. Further physics of how V-shaped antennas work is discussed in Capasso's paper[13].

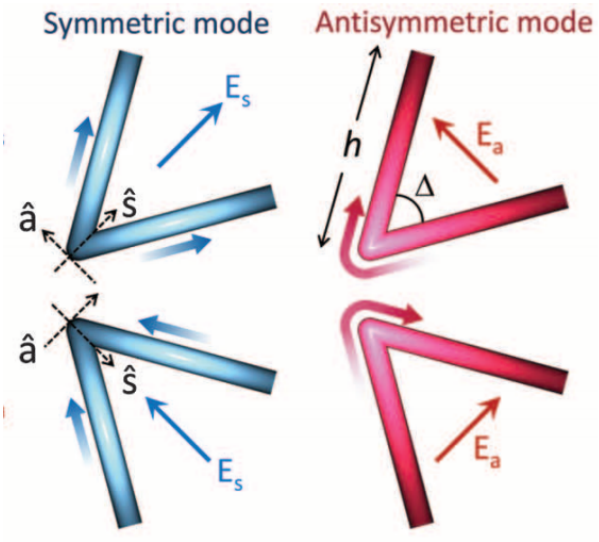

FIG. 9: *A V-antenna with blue referring to symmetric mode and red for anti-symmetric modes along with brighter colour representing larger currents[5]*

B. PB Phase Metasurface

PB phase MS are not very different from multi-resonance MS; the latter is based on varying the geometry of the antennas to achieve variations in phase and amplitude, while, in contrast, the former achieves phase control by adjusting orientation angles of antennas with identical geometries. We can quickly formalize these with Jones matrices to find the transmission coefficients of the rotated system. Consider an anisotropic structure under normal incidence with t_0 and t_e representing the complex transmission coefficients when the polarization of light is along the two principle axes of the nanostructure as shown in

Fig(9). We can immediately calculate the Jones matrix for the system:

$$\begin{aligned}\hat{t}(\theta) &= R(-\theta)\begin{bmatrix} t_0 & 0 \\ 0 & t_e \end{bmatrix} R(\theta) \\ &= \begin{bmatrix} \cos\theta & -\sin\theta \\ \sin\theta & \cos\theta \end{bmatrix}\begin{bmatrix} t_0 & 0 \\ 0 & t_e \end{bmatrix}\begin{bmatrix} \cos\theta & \sin\theta \\ -\sin\theta & \cos\theta \end{bmatrix} \\ &= \begin{bmatrix} t_0\cos^2\theta + t_e\sin^2\theta & (t_0 - t_e)\cos\theta\sin\theta \\ (t_0 - t_e)\cos\theta\sin\theta & t_e\cos^2\theta + t_0\sin^2\theta \end{bmatrix}\end{aligned} \tag{82}$$

If the incident light is CP ($\hat{e}_{L/R} = (\hat{e}_x \pm i\hat{e}_y)/\sqrt{2}$), we can easily calculate the transmitted electric field ($E^t_{L/R}$):

$$E^t_{L/R} = \hat{t}(\theta)\cdot\hat{e}_{L/R} = \frac{t_0 + t_e}{2}\hat{e}_{L/R} + \frac{t_0 - t_e}{2}e^{\pm 2i\theta}\hat{e}_{R/L} \tag{83}$$

It can be seen from Eq(83) that the first term has the same helicity as the incident beam while the second term has opposite helicity from the incident light beam along with an additional PB phase ($\pm 2i\theta$). Hence, the phase shift can be tuned from 0 to 2π for opposite-handedness radiation as the nanostructure is rotated from 0 to 2π.

V. APPLICATIONS

Developments made with metasurfaces have enabled various applications in and out of optics. Many of these MS applications are promising alternatives to replace conventional optical devices since MS are ultrathin, compact and versatile with custom tailoring over amplitude, phase and polarization of light.

A. Metalenses

Metasurfaces can be used to design planar metalenses, which use the basic principle of using spatially varying refractive index over the surface to act as a lens. We must model the phase accumulation over the surface of these devices such that the phase profile converts incident planar wavefronts into circular[14]:

$$\phi(x, y) = -\frac{2\pi}{\lambda}\left(\sqrt{x^2 + y^2 + z^2} - f\right) \tag{84}$$

Where λ is the wavelength in free space, and f is the focal length of the desired lens. However, these metalenses have relatively low efficiency due to weak light coupling to the single-layered plasmonic antennas. In addition to V-shaped nanostructures, U-shaped nanorods have also been used with a similar basis of PB phase manipulation to create metalenses.

Metalenses also serve their purpose in computational imaging. The intensity profiles captured and interpreted in computational imaging are often blurry and not direct images of objects. Attempts have been made to create multi-functional metalenses with structuring point spread functions (PSF), which serve multipurpose edge-enhancing imaging, control phase, and polarization. Full-colour imaging can be achieved by optimizing symmetric PSF and then using neural-network-based image reconstruction.

B. Image processing

The demand for fast and efficient image processing is the need of the hour in various fields, such as object identification, machine vision and artificial intelligence. Metasurface-enabled computing has successfully overcome the analog-to-digital conversion delay. MM-based computing has enabled many computations, such as spatial differentiation, integration, and convulation[15]. It has also enabled differential operations in the Fourier domain via the green function method.

C. Optical Vortex Generation

Metasurfaces applied to optical vortex generation are of immense interest in recent times due to varied applications in high-resolution microscopy, optical tweezers, and classical and quantum communication technology. PB phase metasurfaces consisting of antennas can be rotated about the origin for optical vortex generation, where the rotation rate determines the topological charge of the structure. For example, a metasurface composed of nanoantennas possessing one full rotation of 2π about the origin corresponds to a topological charge of q=1. Due to the rotational invariance of the metasurface, it does not exchange angular momentum with the optical field. Conservation of angular momentum suggests that SAM must be converted into OAM, and hence, this yields a light-carrying OAM of $l = \pm 2q\hbar$.

VI. CONCLUSION

The field of metasurfaces is rapidly progressing with time and possesses enormous scope in various fields, given its vast application. In this paper, we have covered the basics of the field, starting with general concepts like Jones Algebra, Angular Momentum, Geometric phases, etc. We further devised a theory for the interaction of light with metasurface, which included the generalized Snell's Law of refraction and reflection. We further discussed the equations of motion of light in metasurfaces in context with the spin hall effect. Applications and experimental realization of the theory were discussed with a focus on V-shaped antennas.

---

[1] K. Y. Bliokh, F. J. Rodríguez-Fortuño, F. Nori, and A. V. Zayats. Spin–orbit interactions of light. *Nature Photonics*, 9(12):796–808, November 2015.

[2] Yijie Shen, Xuejiao Wang, Zhenwei Xie, Changjun Min, Xing Fu, Qiang Liu, Mali Gong, and Xiaocong Yuan. Optical vortices 30 years on: Oam manipulation from topological charge to multiple singularities. *Light: Science and Applications*, 8:90, 10 2019.

[3] Yachao Liu, Yougang Ke, Hailu Luo, and Shuangchun Wen. Photonic spin hall effect in metasurfaces: a brief review. *Nanophotonics*, 6(1):51–70, 2017.

[4] Shiyi Xiao, Jiarong Wang, Fu Liu, Shuang Zhang, Xiaobo Yin, and Jensen Li. Spin-dependent optics with metasurfaces. *Nanophotonics*, 6(1):215–234, 2017.

[5] Nanfang Yu, Patrice Genevet, Mikhail A. Kats, Francesco Aieta, Jean-Philippe Tetienne, Federico Capasso, and Zeno Gaburro. Light propagation with phase discontinuities: Generalized laws of reflection and refraction. *Science*, 334(6054):333–337, OCT 21 2011.

[6] Alexander V. Kildishev, Alexandra Boltasseva, and Vladimir M. Shalaev. Planar photonics with metasurfaces. *Science*, 339(6125):1232009, 2013.

[7] J. D. Jackson and Ronald F. Fox. Classical electrodynamics, 3rd ed. *American Journal of Physics*, 67(9):841–842, 09 1999.

[8] Subhasish Gupta, Nirmalya Ghosh, and Ayan Banerjee. *Wave Optics: Basic Concepts and Contemporary Trends*. 10 2015.

[9] Les Allen and Miles Padgett. *The Orbital Angular Momentum of Light: An Introduction*, chapter 1, pages 1–12. John Wiley and Sons, Ltd, 2011.

[10] Konstantin Y. Bliokh, Aleksandr Y. Bekshaev, and Franco Nori. Optical momentum, spin, and angular momentum in dispersive media. *Phys. Rev. Lett.*, 119:073901, Aug 2017.

[11] M. V. Berry. Quantal phase factors accompanying adiabatic changes. *Proceedings of the Royal Society of London. Series A, Mathematical and Physical Sciences*, 392(1802):45–57, 1984.

[12] K.Yu. Bliokh and Yu.P. Bliokh. Topological spin transport of photons: the optical magnus effect and berry phase. *Physics Letters A*, 333(3):181–186, 2004.

[13] Nanfang Yu, Francesco Aieta, Patrice Genevet, Mikhail A. Kats, Zeno Gaburro, and Federico Capasso. A broadband, background-free quarter-wave plate based on plasmonic metasurfaces. *Nano Letters*, 12(12):6328–6333, 2012. PMID: 23130979.

[14] Francesco Aieta, Patrice Genevet, Mikhail A. Kats, Nanfang Yu, Romain Blanchard, Zeno Gaburro, and Federico Capasso. Aberration-free ultrathin flat lenses and axicons at telecom wavelengths based on plasmonic metasurfaces. *Nano Letters*, 12(9):4932–4936, 2012. PMID: 22894542.

[15] Haejun Kwon, Ehsan Arbabi, Seyedeh Mahsa Kamali, and Andrei Faraon. Single-shot quantitative phase gradient microscopy using a system of multifunctional metasurfaces. *Nature Photonics*, 14(2):109–114, 2020.